

Engineering Notes

ENGINEERING NOTES are short manuscripts describing new developments or important results of a preliminary nature. These Notes cannot exceed 6 manuscript pages and 3 figures; a page of text may be substituted for a figure and vice versa. After informal review by the editors, they may be published within a few months of the date of receipt. Style requirements are the same as for regular contributions (see inside back cover).

Estimation of Entry Parameters from Heat Flux Measurements

A. K. Alekseev*

ENERGIA Corporation,

Korolev, Moscow Region 141070, Russia
and

G. A. Pavlov†

Russian Academy of Sciences,

Chernogolovka, Moscow Region 142432, Russia

Nomenclature

b	= parameters of atmospheric approximation
comp	= results of computation
CON	= continual mode
C_x	= drag coefficient
e	= boundary-layer edge parameters
exp	= results of experiment
FM	= free molecular flow mode
g	= gravitational acceleration, m/s^2
H	= altitude, km
Kn	= Knudsen number
Nu	= Nusselt number
Q	= heat flux, kW/m^2
R	= radius from planet center, km
Re	= Reynolds number
St	= Stanton number
U	= velocity, m/s
w	= wall conditions
θ	= entry flight-path angle, deg
λ_a	= longitude, deg
λ_i	= eigenvalue
μ	= viscosity, $kg/(m \cdot s)$
ρ	= atmosphere density, kg/m^3
φ	= latitude, deg
ψ	= course angle (velocity projection vs latitude), deg
ω	= planet angular velocity, deg/s
0	= entry parameters at some reference point of trajectory

Introduction

THERE are only three direct measurements of Martian atmosphere parameters (by Viking 1 and 2 and Mars 6 spacecrafts). Usually the vehicle velocity $U(t)$ and altitude are measured by three accelerometers.¹ The same data are used to determine the atmospheric density via vehicle deceleration. The pressure is determined by the atmospheric equilibrium condition

$$P(H) = \int_H^\infty \rho(h)g dh$$

Received June 4, 1996; revision received Dec. 30, 1997; accepted for publication March 6, 1998. Copyright © 1998 by the American Institute of Aeronautics and Astronautics, Inc. All rights reserved.

*Senior Researcher, Department of Aerodynamics and Heat Transfer.

†Leading Researcher, Institute for Chemical Physics.

and the temperature by the state equation. The measurement of atmospheric parameters and velocity by alternative means is of interest also as some supplement to the standard method. For example, the base pressure was considered for this purpose,² although with relatively low accuracy. Direct measurement of velocity and freestream parameters at the high heat flux stage is close to impossible. The simplest measurements at the re-entry are the heat flux (wall temperature) measurements. Herein, the determination of entry parameters from surface heat flux measurements is discussed for the small autonomous station (SAS) that was a member of the MARS-96 program (Fig. 1). The problem was stimulated by the absence of a radionavigational facility for state vector determination before the SAS entered the atmosphere. Because of that, the atmospheric parameters cannot be refined using standard methods.³ The heat flux readings contain nontrivial information on flight conditions. This Note's purpose is to demonstrate that heat flux data can supplement the standard methods for trajectory and atmospheric density estimation.

Input Data

The heating rate to the SAS is determined by freestream parameters $\rho(t)$, $U(t)$, and $T(t)$ and orientation. In general, the heat flux computation needs to solve Boltzmann equations for a rarefied medium and Navier-Stokes equations for a continuous one. We consider events when heat flux can be computed by means of some finite expressions, although it strongly restricts the range of our results' applicability. We consider herein the stagnation point heating rate $Q_w(t)$. The utilization of $Q_w(t)$ is acceptable because angle of attack and roll angle are insignificant for SAS movement.³

Governing Equations

The following model of spacecraft movement is used⁴:

$$\frac{dU}{dt} = g \sin \theta - \frac{C_x S \rho U^2}{2M} + R \omega^2 (\cos \varphi \sin \theta - \sin \varphi \sin \psi \cos \theta) \cos \varphi \quad (1)$$

$$U \frac{d\theta}{dt} = g(R) \cos \theta \left(\frac{U^2}{Rg} - 1 \right) \quad (2)$$

$$\frac{dR}{dt} = -U \sin \theta \quad (3)$$

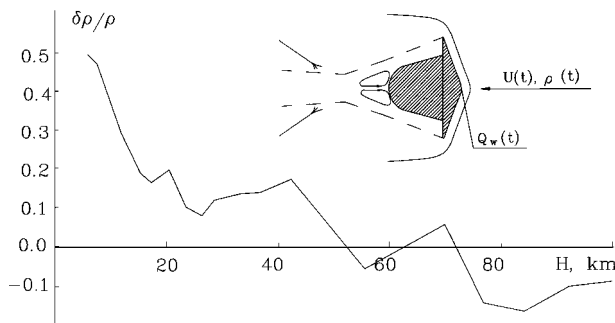


Fig. 1 Relative error of atmospheric density [at $\sigma = 30\%$ in $Q_w(t)$]: $[\rho_{comp}(H) - \rho(H)]/\rho(H)$.

$$U \frac{d\psi}{dt} \cos \psi = -\frac{U^2}{R} t g \varphi \cos^2 \theta \cos \psi \quad (4)$$

$$\frac{d\varphi}{dt} = \frac{U \cos \theta \sin \psi}{R} \quad (5)$$

$$\frac{d\lambda_a}{dt} = \frac{U \cos \theta \cos \psi}{R \cos \varphi} \quad (6)$$

The altitude dependence of density was assumed as follows:

$$\rho(H) = \rho_b \exp(-H/H_b) \quad (7)$$

We should determine H_0 , U_0 , θ_0 , and $\rho(H)$ by minimizing the discrepancy of the following type:

$$\Delta(H_0, U_0, \theta_0, \rho_b, H_b) = \sum_j [Q_w^{\exp}(X_j, t) - Q_w^{\text{comp}}(X_j, t)]^2 \quad (8)$$

The heat transfer was computed with an expression accepted in the following form:

$$\frac{Nu}{Re^{0.5}} = 0.763 \times Pr_w^{0.4} \left(\frac{\rho_e \mu_e}{\rho_w \mu_w} \right)^{0.4} \quad (9)$$

The approach from Ref. 5 was used:

$$St_0 = \frac{St_{\text{CON}} + (Kn/3)^2 St_{\text{FM}}}{1 + (Kn/3)^2}, \quad Kn = \frac{M_\infty}{(Re_\infty)^{0.5}}$$

for heat transfer computations at free molecular and transition modes. This method enables calculation of heat flux for all flow modes from free molecular to continuous.

The matrix

$$M_{ij} = \sum_k \frac{\partial Q(t_k)}{\partial f_i} \frac{\partial Q(t_k)}{\partial f_j}$$

spectrum is used here as a heuristic for singularity and ill-conditioners' detection, although formally it is not applicable because of problem nonlinearity. The matrix $(1/\sigma^2)M_{ij}$ is the Fisher informational matrix. The spectrum of matrix M_{ij} for parameters $f_i = (H_0, U_0, \theta_0, \rho_b, H_b)$ was computed numerically (for SAS conditions):

$$\begin{aligned} \lambda_1 &= 1780.0, & \lambda_2 &= 19.4, & \lambda_3 &= 5.6 \\ \lambda_4 &= 0.4, & \lambda_5 &= 0.04 \end{aligned}$$

The problem is not singular, and it is not ill-conditioned (at this number of parameters) despite large variation of the eigenvalues' magnitude. The usual relative dispersion for heat flux measurements is $\sigma^2 \sim 0.01$ – 0.1 . The value of the minimum eigenvalue is comparable with dispersion of input data $\lambda_5 \sim \sigma^2$. Thus, the effective rank of the problem equations (1–9) equals 5 at realistic measurement errors.

The accuracy of inverse problem results can be estimated by M_{ij} diagonal elements: $\sigma_i^2 \sim \sigma^2/M_{ii}$. The following values of diagonal elements were computed: $M_{11} = 734.0$, $M_{22} = 593.0$, $M_{33} = 454.0$, $M_{44} = 4.2$, and $M_{55} = 16.4$. The accuracy of ρ_b estimation is minimal.

The problem equations (1–9) are, generally speaking, ill-posed. The number of parameters f_i can be considered as the regularization parameter. The natural wish is to increase the number of atmosphere approximation parameters. For the six-parameter problem ($H_0, U_0, \theta_0, \rho_b, H_b, H_{b1}$), the value of the last λ_i rapidly diminishes: $\lambda_6 = 10^{-6}$. For the seven-parameter problem ($H_0, U_0, \theta_0, \rho_b, H_b, H_{b1}, H_{b2}$), the values of last two λ_i are $\lambda_6 = 10^{-2}$ and $\lambda_7 = 4 \times 10^{-8}$. The six- and seven-parameter inverse problem solutions provide the computed density deviation from the exact one about 14 and 30 times, respectively (at input data error $\sigma = 0.1$), and so the maximum volume of information (number of parameters) in the considered problem is strongly restricted.

Table 1 Error in PAET parameters estimation

Parameter:	H_0 , km	U_0 , m/s	θ_0 , deg	$(\delta\rho/\rho)_{\text{max}}$
Result error	3.4	180	2.0	0.5

Table 2 Accuracy of results

Parameter:	H_0 , km	U_0 , m/s	θ_0 , deg
Error for $\sigma = 10\%$	2.6	40	0.02
Error for $\sigma = 30\%$	4.6	200	1.12
Ref. 3 error	± 5	± 30	± 5

Estimation of PAET Entry Conditions

The entry parameters and atmospheric density variation were estimated using measurements on the Planetary Atmosphere Experiments Test (PAET) lander bow shield⁶ for method verification. The PAET trajectory ($H_0 = 90$ km, $U_0 = 6560$ m/s, and $\theta_0 = 40.8$ deg) and shape are similar to those of the SAS. The heat flux was measured on the PAET bow shield at an angle of 19.5 deg from the critical point. The entry and atmosphere parameters were estimated using $Q_w(t)$ with the error shown in Table 1. The maximum density deviation obtained using accelerometers⁶ was $(\delta\rho/\rho)_{\text{max}} = 0.2$.

Estimation of SAS Entry Conditions

The numerical experiments on the SAS were performed with the following approach. The descent trajectory and heat flux $Q_{\text{cr}}(t)$ were computed for the set of entry parameters³ $H_0 = 100$ km, $U_0 = 5600$ m/s, and $\theta_0 = 16.0$ deg and the atmospheric parameters 40°N (40° of north latitude and 0-nominal altitude of surface).⁷ The value $Q_{\text{cr}}(t)$ imitated the experimental data. According to Ref. 8, expression (9) works for CO₂ atmosphere with acceptable accuracy (in CO₂ the heat flux is 5–6% higher). Gauss error of dispersion $\sigma = 1$ –30% was added to $Q_w(t_i)$ for experimental noise imitation. The optimization problem [Eq. (8)] was solved with the Nelder–Mead⁹-type method. The error in parameter estimation is presented in Table 2. The relative error in density profile at $\sigma = 30\%$ is presented in Fig. 1. The heat flux data in the SAS stagnation point are sufficient for the estimation of both the entry parameters H_0 , U_0 , and θ_0 and two atmospheric parameters.

Concluding Remarks

Heat flux at the spacecraft surface contains the information sufficient to estimate some set of trajectory and atmospheric parameters. The stagnation point data are sufficient for solution of the five-parameter problem with realistic heat flux errors. The treatment of PAET flight data confirms the possibility of entry and atmospheric parameter estimation using stagnation point heat flux. Thus, this method can be considered as a supplemental one for some special cases when deceleration data are absent.

The accuracy can be partly improved by using more sophisticated numerical methods of computational fluid dynamics for heat flux estimation. The accuracy in heat flux measurements and computations above 15–20% looks unrealistic. Some improvement can be achieved by utilization of data from different zones of landers (stagnation point and conical part).

References

- Seiff, A., "Atmospheres of Earth, Mars, and Venus as Defined by Entry Probe Experiments," *Journal of Spacecraft and Rockets*, Vol. 28, No. 3, 1991, pp. 265–276.
- Cassanto, J. M., "A Base Pressure Experiment for Determining the Atmospheric Pressure Profile of Planets," *Journal of Spacecraft and Rockets*, Vol. 10, No. 4, 1973, pp. 253–261.
- Ivankov, P. R., "A Robust Method for Small Station Descent Trajectory Restoration," *Space Researches*, Vol. 33, No. 5, 1995, pp. 533–535.
- Neyland, V. Y., and Tumin, A. M., "Aerothermodynamics of Atmosphere-Space Planes," TcAGI, Zhukovsky, Russia, 1991 (in Russian).
- Nomura, S., "Correlation of Hypersonic Stagnation Point Heat Transfer at Low Reynolds Numbers," *AIAA Journal*, Vol. 12, No. 12, 1983, pp. 1598–1600.
- Vojvodich, N. C., "PAET Entry Heating and Heat Protection Experiment," *Journal of Spacecraft and Rockets*, Vol. 10, No. 3, 1973, pp. 181–189.

⁷Moroz, B. I., Kerganovich, V. V., and Krasnopol'skiy, V. A., "Martian Atmosphere Model for MARS-94 Project (MA-90)," *Space Researches*, Vol. 29, No. 1, 1991, pp. 3-84.

⁸Tauber, M. E., Bowles, J. V., and Yang, L., "The Heating Environment During Martian Atmospheric Descent," *Journal of Spacecraft and Rockets*, Vol. 26, No. 5, 1989, pp. 330-337.

⁹Nelder, I., and Mead, R., "A Simplex Method for Function Minimization," *Computer Journal*, Vol. 7, 1965, pp. 308-313.

T. C. Lin
Associate Editor

Unity Check Method for Structural Damage Detection

Cheng S. Lin*
The Aerospace Corporation,
El Segundo, California 90245-4691

Introduction

IN anticipation of the deployment of large structures in space, researchers have been trying to develop methods to detect and to locate structural damage if it occurs. One promising approach is to use modal data collected from an on-orbit mode survey test to detect critical damage. Damage in the structure causes degradation in its stiffness properties, which in turn changes its mode shapes and frequencies. Assuming that a finite element model has been developed and verified by an earlier mode survey test before damage occurs, the problem of using measured modes and frequencies from a later mode survey test to detect damage is equivalent to trying to correct a defective finite element model using mode survey test data.

Several researchers have developed different methods to locate the physical positions of modeling errors.¹⁻⁴ The author has proposed a unity check method to locate modeling errors in stiffness using modal test data.⁵ This Note applies the method to locate structural damage and, furthermore, to determine the magnitudes of stiffness reduction in the damaged elements by the least-squares technique. It is assumed that the analytical model of the original structure has been satisfactorily verified by a mode survey test.

Theoretical Formulation

It can be proved that the following relationships are true for an n -degree-of-freedom linear dynamic system⁵:

$$[K] = [M] \left(\sum_{i=1}^n \omega_i^2 \{\phi_i\} \{\phi_i\}^T \right) [M] \quad (1)$$

$$[f] = [\phi] [\omega^{-2}] [\phi]^T = \sum_{i=1}^n \omega_i^{-2} \{\phi_i\} \{\phi_i\}^T \quad (2)$$

where $[K]$, $[f]$, and $[M]$ are the stiffness, flexibility, and mass matrices, respectively; ω_i is the i th modal frequency; $\{\phi_i\}$ is the i th modal vector; $[\phi]$ is the modal matrix; and $[\omega]$ is the modal frequency matrix. From Eq. (1), it can be seen that modal contribution to the stiffness matrix increases as the modal frequency increases, whereas Eq. (2) reveals that the flexibility matrix converges rapidly as the frequency increases.

In the mode survey test for the potentially damaged structure, only the lowest few modes can be accurately measured because of

instrument limitation. Therefore, the flexibility matrix for the damaged structure can be best approximated by the following partitioned expression:

$$[f_d] = [\phi_{ld} \ \phi_{hu}] \begin{bmatrix} \omega_{ld}^{-2} & \\ & \omega_{hu}^{-2} \end{bmatrix} [\phi_{ld} \ \phi_{hu}]^T \quad (3)$$

where subscripts d and u denote the damaged and undamaged structure, respectively; subscripts l and h indicate the lower and higher modes, respectively. The stiffness matrix for the damaged structure is

$$[K_d] = [K_u] - [\Delta K] \quad (4)$$

where $[\Delta K]$ is the changes in stiffness due to the damage. By definition,

$$[f_d][K_d] = [I] \quad (5)$$

Substituting Eq. (4) into Eq. (5), one obtains the following:

$$[f_d][\Delta K] = [E] \quad (6)$$

where

$$[E] = [f_d][K_u] - [I] \quad (7)$$

Because $[\Delta K]$ results from the damage, it will have nonzero values only at degrees of freedom connected to the damaged members. Therefore, Eq. (6) can be partitioned as follows:

$$\begin{bmatrix} \bar{f}_{da} & \bar{f}_{db} \end{bmatrix} \begin{bmatrix} 0 & 0 \\ 0 & \Delta \bar{K} \end{bmatrix} = \begin{bmatrix} \bar{E}_a & \bar{E}_b \end{bmatrix} \quad (8)$$

where $\Delta \bar{K}$ is the nonzero submatrix of $[\Delta K]$, \bar{f}_{da} and \bar{f}_{db} are submatrices of $[f_d]$, and \bar{E}_a and \bar{E}_b are submatrices of $[E]$. It can be seen that \bar{E}_b will have significant values and \bar{E}_a will not. Furthermore, the error of each degree of freedom can be measured by the maximum absolute value of elements in the corresponding column of $[E]$, namely,

$$\varepsilon_j = \max_{i=1}^n |e_{ij}| \quad (9)$$

By inspecting the magnitudes of ε_j , one can identify the affected degrees of freedom.

Dropping the subscript b in \bar{f}_{db} and \bar{E}_b for simplicity, Eq. (8) can be simplified as follows:

$$\begin{bmatrix} \bar{f}_d & \Delta \bar{K} \end{bmatrix} = \begin{bmatrix} \bar{E} \end{bmatrix} \quad (10)$$

$n \times l \quad l \times l \quad n \times l$

where l is the total number of affected degrees of freedom. Because $[\bar{f}_d]$ and $[\bar{E}]$ are known, Eq. (10) represents a set of linear constraints for the elements of $[\Delta \bar{K}]$. To facilitate the solution for $[\Delta \bar{K}]$, Eq. (10) is transformed into the standard form for a system of overdetermined simultaneous equations as follows:

$$\begin{bmatrix} \bar{f}_d & \Delta \hat{K} \end{bmatrix} = \begin{bmatrix} \hat{E} \end{bmatrix} \quad (11)$$

$nl \times ll \quad ll \times l \quad nl \times l$

where

$$[\tilde{f}_d] = \begin{bmatrix} \bar{f}_d & 0 & \cdots & 0 \\ 0 & \bar{f}_d & \cdots & 0 \\ \vdots & \vdots & \ddots & \vdots \\ 0 & 0 & \cdots & \bar{f}_d \end{bmatrix} \quad (12)$$

and where $[\Delta \hat{K}]$ and $\{\hat{E}\}$ are column vectors formed by stacking columns of $[\Delta \bar{K}]$ and $[\bar{E}]$, respectively. Furthermore, from the affected degrees of freedom and their connectivity, one can identify the structural members that may have been damaged. Such identification does not have to be exclusive. In the succeeding numerical

Received Aug. 5, 1997; revision received March 30, 1998; accepted for publication April 6, 1998. Copyright © 1998 by the American Institute of Aeronautics and Astronautics, Inc. All rights reserved.

*Engineering Specialist, Structural Dynamics Department, 2350 E. El Segundo Boulevard. Senior Member AIAA.